



# IJCSI

## International Journal of Computer Science Issues

**An Automated Intelligent Approach for ECG Signal Noise  
Removal**

**By Sara Moein, Rajasvaran Logeswaran and Khazaimatol Shima Subari**

**Volume 2, 2012  
ISSN (Online): 1694-0814**

**© IJCSI PUBLICATION  
[www.IJCSI.org](http://www.IJCSI.org)**

IJCSI proceedings are currently indexed by:



Cogprints

Google scholar



SciRate.com

CiteSeer<sup>x</sup> beta



Q·Sensei BETA

DOAJ DIRECTORY OF OPEN ACCESS JOURNALS



ProQuest



© IJCSI PUBLICATION 2012

www.IJCSI.org

# AN AUTOMATED INTELLIGENT APPROACH FOR ECG SIGNAL NOISE REMOVAL

Copyright © 2012 by Sara Moein, Rajasvaran Logeswaran and Khazaimatol Shima Subari

All rights reserved. No part of this thesis may be produced or transmitted in any form or by any means without written permission of the author.

ISSN(online) 1694-0814

© IJCSI PUBLICATION 2012

[www.IJCSI.org](http://www.IJCSI.org)

# **An Automated Intelligent Approach for ECG Signal Noise Removal**

**Sara Moein, MSc,  
Rajasvaran Logeswaran, PhD,  
and Khazaimatol Shima Subari, PhD**

*Faculty of Engineering, Multimedia University  
63100 Cyberjaya, MALAYSIA*

---

**Corresponding author:**

Sara Moein  
Faculty of Engineering, Multimedia University, 63100 Cyberjaya, Malaysia  
Tel. +6017-3553894  
[Sara.moein08@mmu.edu.my](mailto:Sara.moein08@mmu.edu.my)

**Abstract**

Electrocardiogram (ECG) is an important biomedical tool for the diagnosis of heart disorders. However, the signal is susceptible to noise and it is essential to remove the noise especially when undertaking automated processing of the signal. In this paper, an intelligent approach based on moving median filter and Self-Organizing Map (SOM) neural network is proposed to identify the cutoff frequency of the noise, which is to be filtered out. In general, the spectrum of the ECG signal is derived, subsequently, baseline wander is removed using the moving median filter and finally, SOM is applied to the spectrum to calculate the cutoff frequency. The results of the proposed scheme are compared with the low-pass FIR filtering for ECG signal high frequency noise removal. Results show that using the proposed intelligent method, the calculated cutoff frequency will be equal or better than the classical results for ECG noise removal. Also, in all the cases of atrial fibrillation, arrhythmia and supraventricular ECG signals, the automatically calculated cutoff frequency produces very smoother signals than the classical low-pass filtering.

**Keywords:** Frequency spectrum, Cutoff frequency, Self-Organizing Map, Low-pass filtering, Finite Impulse Response (FIR).

## I. Introduction

An effective way to detect heart disorders is through the analysis of the electrocardiogram (ECG) signals [1]. The ECG signal is generated by polarization and depolarization of the heart that occurs when pumping blood throughout the human body, and it can be recorded by contacting electrodes to the skin at specific locations on the body. The ECG signal waveform consists of the P wave, QRS wave and T wave, as shown in Fig. 1. In the overall ECG interpretation for computerized interpretation programs and for the human electrocardiographer, it is vital to access accurate measurements of ECG intervals and axes (P/ QRS/ T) [2].

The recorded ECG signal usually contains noise, which includes low-frequency components that cause baseline wander, and high-frequency components such as power-line interference [3]. The sources of noise effecting ECG signals include imperfect contact of electrodes to the body, machine malfunction, electrical noise from elsewhere in the body, respiration and muscle contraction [4]. The presence of noise corrupts the signal, and ECG signal processing systems need to be equipped with the ability to remove the noise in order to do any analysis on the signal. In noise removal, it is necessary to identify the cutoff frequency of the filter. However, it is difficult to determine this threshold, in which the exact value often varies between signals. Inaccurate thresholds will erase important information in the signal.

There have been several studies on ECG signal noise removal [5-11]. Zhang and Sui [5] proposed a method based on morphological filtering and wavelets to eliminate the noise in ECG signals and increase the diagnosis efficiency. In their method, the morphological filter is used to filter out the baseline interference signal,

and the wavelet transform is applied to remove high frequency interference. Another study was the novel noise-filtering algorithm by Chang [6], which is based on ensemble empirical mode decomposition (EEMD) to remove artifacts in ECG traces. Three noise patterns with different characteristics - 50 Hz, Surface electromyograms (EMG), and base line wander - were embedded into simulated and real ECG signals. The mean square error (MSE) between clean and filtered ECGs was used as the filtering performance index. Results showed that high noise reduction is the major advantage of the EEMD based filter, especially on arrhythmia ECGs. In another study, Ling et al. [7] proposed some fuzzy rules for formulating and integrating different multiwavelets with pre- and post- filters to incorporate expert knowledge at different noise levels.

Poungponsri and Yu [8] used the wavelet neural network (WNN) for ECG signal modeling and noise reduction. WNN combines the multiresolution nature of wavelets and the adaptive learning ability of artificial neural networks (ANN), and is trained by a hybrid algorithm that includes the Adaptive Diversity Learning Particle Swarm Optimization (ADLPSO) and the gradient descent optimization. Sotos et al. [9] presented a noise cancellation system suitable for different biomedical signals based on a multilayer ANN. The proposed method consists of a simple structure similar to the MADALINE neural network (Multiple ADaptive LINear Element). In [10], Sotos et al. worked on removing the baseline drift using ANN. The results obtained showed that the ANN-based approach performs better, with respect to baseline drift reduction and signal distortion at the filter output, than traditional methods.

Although there are many new methods for noise removing, many noise removal systems for ECG signals still use the band-pass filter because of simplicity in

implementation and less number of required coefficients [11-17]. The important consideration of this popular technique is in automatically identifying the correct pass bands in the frequency spectrum. Note that for filters concerned with noise removal, there is insufficient research in the area of automated calculation of the cutoff frequencies. This paper proposes a scheme that can automatically identify the cutoff frequency for implementation of the FIR. In this study, FIR is preferred to the infinite impulse response (IIR) filter because IIR filters are more susceptible to problems of finite-length arithmetic. Additionally, FIR filters are easier to implement. More information on FIR filters may be found in [18].

Previous research has indicated that the ANN presents effective approaches for denoising signals. Therefore, in this paper, we present a method using SOM, an unsupervised ANN, to automatically calculate the cutoff frequency. The proposed scheme is discussed in more detail in the next section, followed by a discussion on the results.

## **II. Materials and Methods**

The proposed method is based on clustering the frequency spectrum using SOM. Fig. 2 shows the flow of the proposed method. The Physiobank archive of ECG signals [19], available for use by the biomedical research community, is used to test the proposed approach. The ECG signals obtained were selected from four databases: the MIT-BIH Supraventricular Arrhythmia Database, the MIT-BIH Normal Sinus Rhythm Database and the MIT-BIH Atrial Fibrillation Database, all sampled with a sampling frequency of 250 Hz, and the MIT-BIH Arrhythmia Database with signals sampled at 360 Hz.

### **A) Baseline Drift Attenuation**

Analysis of typical ECG signals indicates that baseline wander is the prominent phenomenon and its distribution and magnitude varies between different signals. An example is given in Fig. 3. The original ECG signal is shown in Fig. 3(a), where the cycles of the PQRST waveform appear to be attenuated by a sinusoidal waveform. The first step in noise reduction is to attenuate the baseline drift. In previous research [20-22], the high-pass filter is used to attenuate the drift of baseline. The applied cutoff frequency for high-pass filtering is 1 Hz [21, 22]. Fig. 3(d) shows the ECG signal after low frequency noise reduction with the FIR high-pass filter. Since the moving median filter is more efficient for baseline drift attenuation and in some cases, the high-pass filter causes ST segment distortion [20], the moving median filter is applied in this work to accomplish this. A moving median filter takes a set of points, and given a span for the filter, takes a subset of those points, and returns the median for the subset. Fig. 3(c) shows the extracted baseline. The resulting effect of baseline drift removal is given in Fig. 3(e), where the baseline wander is eliminated (i.e., virtual straight line at 0 amplitude).

### **B) Application of FIR Filtering**

After attenuation of the baseline drift, the high amplitude noise is removed. In order to obtain the spectrum of the ECG signal, it is transformed to the frequency domain using the Fast Fourier Transform (FFT) defined as follows:

$$X_k = \sum_{n=0}^{N-1} x_n e^{-i2\pi k \frac{n}{N}} \quad \text{for } k = 0, \dots, N-1 \quad (1)$$

where  $X_0, \dots, X_{N-1}$  are complex numbers.

The implementation of the FIR filter requires three parameters: a cutoff frequency ( $\omega_c$ ), the filter order ( $N$ ), and the window type ( $w$ ). The filter order primarily determines the width of the transition band. Higher orders give sharper cutoff in the frequency response [18]. Therefore, the desired sharpness will determine the filtering order. A hamming window of size  $N+1$  is used in the FIR filter, as given by Eq. (2).

$$w_n = 0.54 - 0.46 \cos(2\pi \frac{n}{N}) \quad \text{for } 0 \leq n \leq N \quad (2)$$

The cutoff frequency is normalized as follows:

$$\omega = \frac{\omega_c}{f_s} \quad (3)$$

where  $\omega$  is the normalized cutoff frequency and  $f_s$  is the sampling frequency.

Fig. 3(b) shows the frequency spectrum up to half of the sampling frequency, which is 360 Hz for the selected ECG signal. As mentioned previously, this study focuses on an intelligent approach for finding this cutoff using SOM neural network.

### C) Clustering of ECG Frequency Spectrum Using SOM

SOM is an unsupervised learning algorithm for modeling the structure of a sample set of patterns [23]. Commonly, SOM is a two-layer neural network: the first being the input layer and the second the competitive layer. The nodes of the first layer selectively feed input elements into the competitive layer of the network. There is a weight vector, which is assigned to each node in the input and competitive layers. Training cycles start with randomly chosen weights for the nodes in the competitive layer [24]. During each training cycle, every input vector is considered in turn and the winner node is determined based on Euclidean distance between the weight vector  $w_i$  and the input vector  $x_i$  such that:

$$\|x_v - w_i\| = \min \|x_v - w_i\| \quad \text{for } i = 1, 2, \dots, N \quad (4)$$

where  $\| \cdot \|$  indicates Euclidean distance, and  $x_v$  indicates the input vector.

The weight vectors of the winning node and the nodes in the neighborhood are updated using a weight adaptation function based on the following Kohonen rule:

$$\Delta w_i = \alpha(x_v - w_i^{old}) \quad \text{for } i \in N_r \quad (5)$$

where  $\alpha$  is the learning coefficient,  $w_i^{old}$  is the weight vector before updating, and  $N_r$  is the collection of all nodes in the neighborhood of radial distance  $r$  from the input layer.

In general, the proposed method clusters the ECG frequency spectrum. The input data consists of typical forms of spectrums for four classes of ECG signals, namely the normal sinus rhythm, supraventricular, atrial fibrillation and arrhythmia. The critical parameter is the number of clusters for configuration of the SOM. The classical geometric method is a well-known technique, which consists of plotting the value of the clustering criterion, and assessing the plot by analyzing discontinuities in the slope [25]. Sharp steps in the curve determine the boundaries of the clusters. Based on analysis of the classical geometric method on the database, it was deduced that the adequate number of clusters was four for each spectrum. This is seen in Fig. 4, which shows typical shapes for the spectrums of the four classes of ECG signals. In the figure, the thick black lines indicate the boundaries of the range of amplitudes for each cluster. The typical ranges for the clusters of the ECG signal were found to be as given Table 1. The ranges may vary a little for spectrums in each class. However, the number of clusters was determined to be four for all spectrums.

Therefore, the SOM is configured with a competitive layer with a  $1 \times 4$  one-dimensional map. The FFT of the ECG signals is the input vector that will be fed to the competitive layer of the SOM. After training, all samples will be clustered in  $c_i = i, (i = 1..4)$ . Fig. 5 shows three ECG signals based on different shapes and characteristics after baseline drift attenuation and the clustering results of FFT using SOM. Since the low amplitude noise are mostly gathered in the lowest cluster,  $c_1$ , then the cutoff frequency is the point that  $c_1 = 1$  changes to  $c_2 = 2$  through right to left scanning of the FFT samples.

It is important to note that there must be stability in the clusters when selecting the cutoff frequency. The stability is determined by defining a left neighborhood

border for each sample. In the right to left scanning of the spectrum, the samples are considered stable in a cluster if:

$$\forall s_i \in c_2 : \delta = 10 \Rightarrow n \geq 4 \quad (6)$$

where  $s_i$  is the sample of clustered FFT,  $\delta$  is the left neighborhood border. Based on empirical results the optimum values for  $\delta$  was found to be 10 samples  $n : n \in c_2$  is the number of the consecutive samples at  $\delta$ .

Experimental results show that four is the adequate number of samples for determining the cutoff frequency. In other words, the cutoff frequency is where there are more than 4 neighboring samples in  $c_2 = 2$  for  $\delta = 10$  through scanning from right to left of the frequency spectrum. For example, in Fig. 5(b) when scanning from right to left, one encounters a single point first, and since it is less than 4, the mentioned single point is ignored and scanning should be continued until reaching the next set of points. Another example is shown in Fig. 5(c), which has more single points that are ignored. Again, the scanning process is continued in order to reach to the stable cluster with the mentioned conditions i.e.,  $\delta = 10 \Rightarrow n \geq 4$ . The obtained frequency  $\omega_c$  is then normalized by Eq. (3).

Investigation on the output of the first stable point identified still showed influence of noise, as seen in Fig. 6(b). To overcome this noise (possibly due to equipment/transmission), the next stable point is used. As observed in Fig. 6(c), this cutoff frequency enables a cleaner signal to be extracted by the FIR filter.

### III) Experiments and Results

A total of 100 ECG signals were randomly selected from the various classes of databases for testing the performance of SOM in identifying  $\omega_c$  using the proposed method. The outcome of scanning the clustered frequency spectra are normalized as described in the pervious section. The automated  $\omega_c$  obtained by the SOM for 20 of the ECG signals is given in table 2. The table shows that even for similar types of heart disorders, there is a significant difference between the cutoff frequencies of the ECGs, further emphasizing the difficulty in automatic identification of the optimum cutoff frequency. Once the cutoff frequency has been determined, the test signals are denoised using the FIR filter.

Figs 7 to 10 present 4 examples of ECG signals with different shapes and characteristics from the mentioned databases. The automatically denoised signals are shown in part (b) of Figs 7-10. To illustrate the denoising effected more clearly, part of the signal is zoomed on the right of the images. As seen from results, a smooth signal is obtained for each type of disorder. The results of FIR filtering by the calculated cutoff frequency are compared with the results of FIR low-pass filtering based on previous studies [13-16]. In these studies, the cutoff frequency for the ECG low-pass filtering was 100 Hz, where all frequencies above 100 Hz are eliminated to remove power-line interference. For fairness in evaluation, the baseline drift has been attenuated for all the test signals using the moving median filter, instead of just using a 1 Hz high-pass filter as per the norm, since it is has been shown in Fig. 3 that the moving median filter is better suited for baseline wander removal. The results of the classical filtering after baseline wander removal are given in part (c) of Figs 7-10. Using the proposed method, the calculated cutoff frequency has been found to be

equal or better than the classical results for ECG noise removal. Comparing the results, it is seen that in all the cases of atrial fibrillation, arrhythmia and supraventricular ECG signals, the proposed intelligent calculated cutoff frequency, produced better results than the classical low-pass filter.

In order to properly design the filter, the cutoff frequency for each type of ECG signal should be known and without eliminating signal information, it is impossible to completely remove the noise. In addition, the cutoff frequency is dynamic. Therefore, for various ECG signals, the cutoff frequency would be different due to the biometric characteristics of the ECG signal. In [26, 27], the ECG signals varied from person to person. Therefore, it is obvious that the frequency spectrum would be different for each person and the applied cutoff frequency has to vary, instead of being fitted as in the classical low-pass filter where 100 Hz is used as the constant threshold. To better evaluate the proposed scheme, visual identification of the optimum cutoff frequency was undertaken. The cutoff frequencies for the best visual results (up to the point just before peak amplitudes were negatively affected) were identified and the results are shown in part (d) of Fig.s 7-10.

The visual cutoff frequencies (Visual  $\omega_c$ ) is also given in comparison with the automated cutoff frequencies in the table indicates that, the difference between the automatically determined cutoff frequency and that of the visual examination is small, as given by the MSE. Thus, the viability of the proposed method in correctly determining the cutoff frequency automatically is further supported.

#### **IV) Conclusion**

In this study, an intelligent approach based on identifying the cutoff frequency using SOM for ECG low-pass filtering is proposed. The results show that the proposed approach is successful and promising. The results present that the identified cutoff frequency is accurate and better than the conventional method as the SOM-based approach works on each signal individually. Examples of atrial fibrillation, arrhythmia and supraventricular ECG signals show that the low-pass filtering with the automated calculated cutoff frequency generates smoother signal. Also, no loss of data is encountered in the denoised signal during the ECG low-pass filtering.

## V) References

1. Karl G. R., Isis A.W., Roberto L., Håkan N., Fetal ECG waveform analysis, *Best Practice & Research: Clinical Obstet Gynae*, 2004; 18:3, pp. 485-514.
2. Robert M., Ian R.G. The effects of noise on computerized electrocardiogram measurements, *J Electrocardiol* 2006; 39:4, pp.165-173.
3. Behbahani S., Investigation of adaptive filtering for noise cancellation in ECG signals, 2nd Intl Multi-Symp Comp Comput Sci, IEEE Computer Society, 2007; pp. 144-149.
4. Fitzgibbon E., Berger R., Tsitlik J., Halperin HR., Determination of the noise source in the electrocardiogram during cardiopulmonary resuscitation, *Med Care Medicine*, 2002; 30:4, pp. 148-153.
5. Zhang D., Sui W., Noise Reduction of ECG Signal Based on Morphological Filtering and WT, *Key Eng Mat*, 2010; 439-440, pp. 12-16.
6. Chang K.M., Arrhythmia ECG Noise Reduction by Ensemble Empirical Mode Decomposition, *Sensors in Biomechanics and Biomedicine*, 2010; pp. 6064-6080.
7. Ling B.W.K., Ho C.Y.F., Lam H. K., Wong T.P.L., Chan Al.Y.P, Tam P.K.S. , Fuzzy rule based multiwavelet ECG signal denoising, *IEEE World Cong Comput Intell*, Hong Kong, 2008; pp. 1064-1068.
8. Pongponsri S., Yu X.H., Electrocardiogram (ECG) signal modeling and noise reduction using wavelet neural networks, *Proceedings of the IEEE Intl Conf Autom Logistics*, Shenyang, China, 2009; pp. 394-398.

9. Sotos J.M., Meléndez C.S., Salort C.V., Abad R.C., Ibáñez J.J.R., A learning based Widrow-Hoff Delta algorithm for noise reduction in biomedical signals, *Bio-inspired Modeling of Cognitive Tasks, LNCS*, 2007; 4527, pp. 377-386.
10. Sotos J.M., Sanchez C., Mateo J., Alcaraz R., Vaya C., Rieta J.J., Neural networks based approach to remove baseline drift in biomedical signals, *11th Mediterr Conf Med Biomed Eng Comput 2007 IFMBE Proc*, 2007;16:2, pp. 90-93.
11. Losada R.A., Design finite impulse response digital filters, Part II. *Microwaves & RF*, 2004; 43, pp. 70-84.
12. Orfanidis S.J., *Introduction to Signal Processing*, Upper Saddle River, New Jersey: Prentice Hall; 1996.
13. Lian Y., Hoo P.C., Digital elliptic filter application for noise reduction in ECG signal, *WSEAS Trans Electron*, 2006; 3:1, pp. 65-70.
14. Engin M., ECG beat classification using neuro-fuzzy network, *Pattern Recogn Lett*, 2004; 25:15, pp. 1715-1722.
15. Minami K., Nakajima H., Toyoshima T., Real-time discrimination of ventricular tachyarrhythmia with Fourier transform neural network, *IEEE Trans Biomed Eng*, 1999; 46:2, pp. 179–185.
16. Lin H., Wensheng H., Xiaolin Z., Chenglin P., Recognition of ECG patterns using artificial neural network, *Proceedings of the Sixth IEEE Intl Conf Intell, Sys Design and Appl (ISDA'06)*, Jinan, 2006; pp. 477-481.
17. Naghsh-Nilchi A.R., Kadkhodamohammadi A.R., Cardiac arrhythmias classification method based on MUSIC morphological descriptors, and neural network, *EURASIP J Adv Sig Process*, (2008), 2008, Article ID 935907.

18. Saramaki T., Mitra S.K., Finite impulse response filter design, Handbook for Digital Signal Processing, New York, New York: Wiley-Interscience; 1993.
19. Physionet, Physiologic signal archives for biomedical research, A database for heart signals, Cambridge, MA, (Updated: 27. April. 2009) [www.physionet.org/physiobank](http://www.physionet.org/physiobank), [accessed on: 10. September. 2010].
20. Roger A., Hans-Jakob S., Meet the challenge of high-pass filter and ST-segment requirements with a DC-coupled digital electrocardiogram amplifier, J Electrocardiol, 2009; 46:6, pp. 574-579.
21. Ziarani A.K., Konrad. A., A nonlinear adaptive method of elimination of power line interferences in ECG signals, IEEE Trans Biomed Eng, 2004; 49:6, pp. 540-547.
22. Willems J.L., Arnaud P., A reference data base for multi-lead electrocardiographic computer measurement programs, J Am Coll Cardiol, 1987; 10:6, pp. 1313-1321.
23. Sordo M., Introduction to Neural Networks in Healthcare, OpenClinical: Knowledge Management for Medical Care, Harvard; 2002.
24. Hassoun M.H., Fundamentals of Artificial Neural Network, MIT; 1995.
25. Hardy A., On the number of clusters, Computational Statistics & Data Analysis, 1996; 23:1, pp. 83-96.
26. Sornmo L., Laguna P., Bioelectrical Signal Processing in Cardiac and Neurological Applications, Academic Press, 688 pages; 2005.
27. Konstantinos N.P., Dimitrios H., Jimmy K.M.L., ECG biometric recognition without fiducial detection, Biometric Consortium Conference, IEEE Biometrics Symp, Baltimore, MD; 2006.

## List of Figures

- Fig. 1. A typical waveform of ECG signal
- Fig. 2. Flow chart of the proposed method
- Fig. 3. ECG signal drift attenuation
- Fig. 4. Four typical ranges of amplitude for frequency spectrum in four classes of ECG
- Fig. 5. Clustering the frequency spectrum
- Fig. 6. Denoising by SOM based on the stable point
- Fig. 7. Arrhythmia ECG signal
- Fig. 8. Supraventricular ECG signal
- Fig. 9. Another supraventricular ECG signal
- Fig. 10. Atrial fibrillation ECG signal

## List of Tables

- Table1. Typical Ranges of Amplitude for the four classes of ECG
- Table 2. Results of SOM for identifying the cutoff frequency

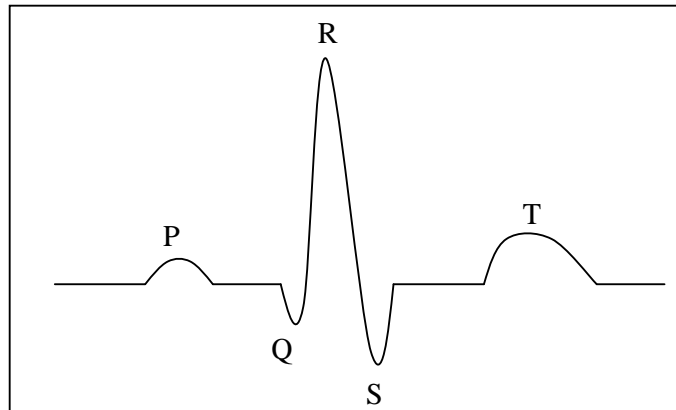


Fig. 1. A typical waveform of ECG signal

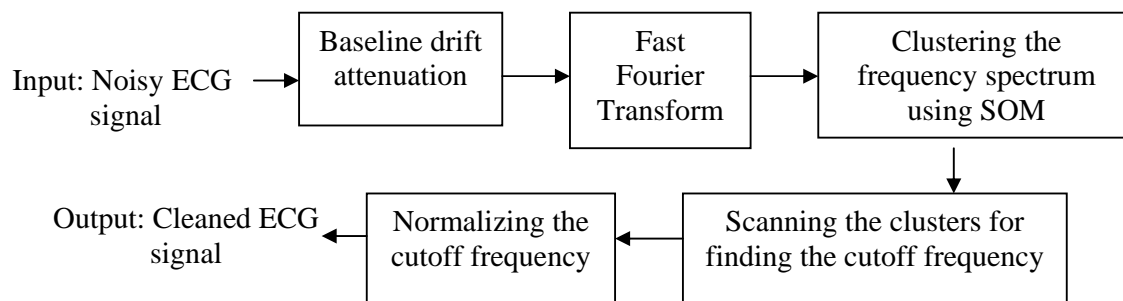


Fig. 2. Flow chart of the proposed method

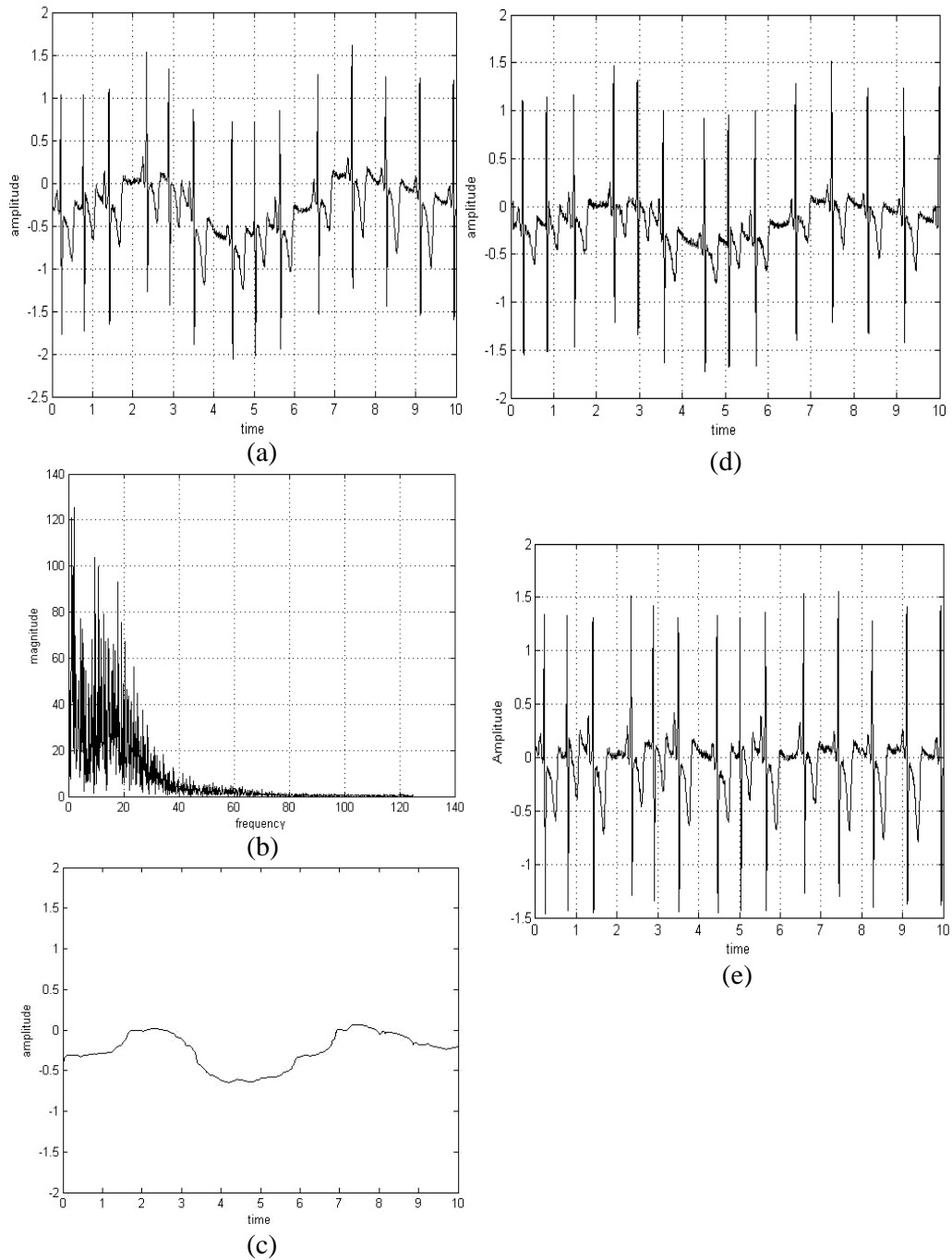
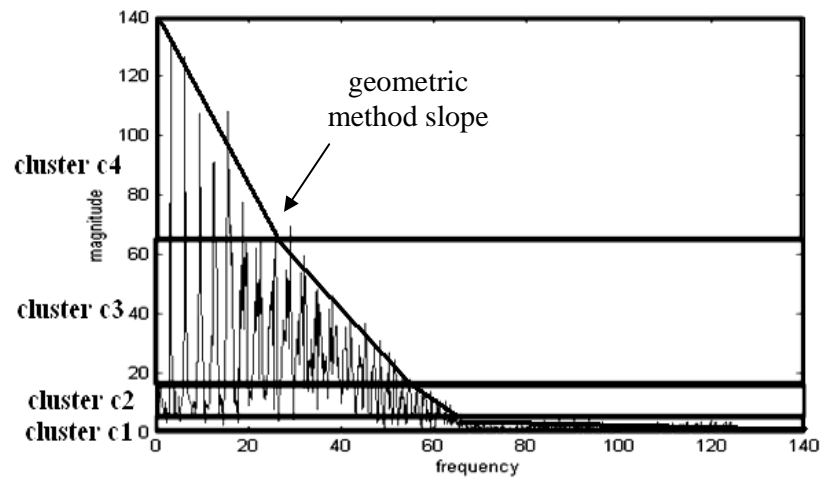
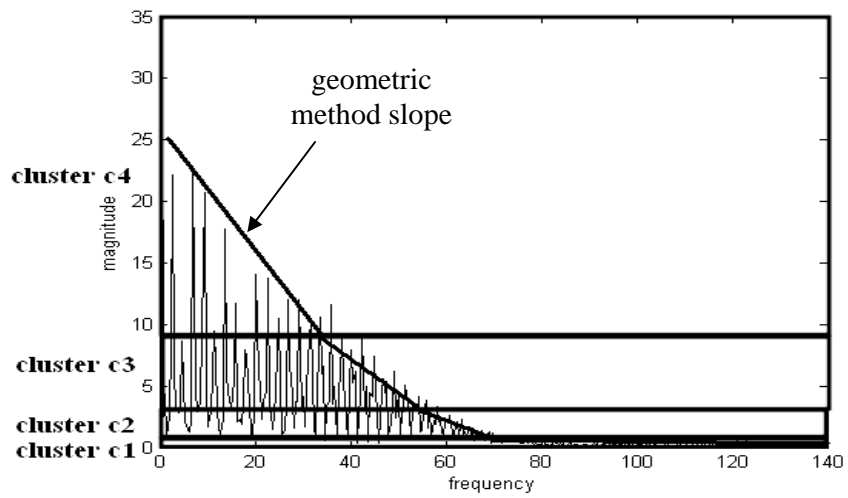


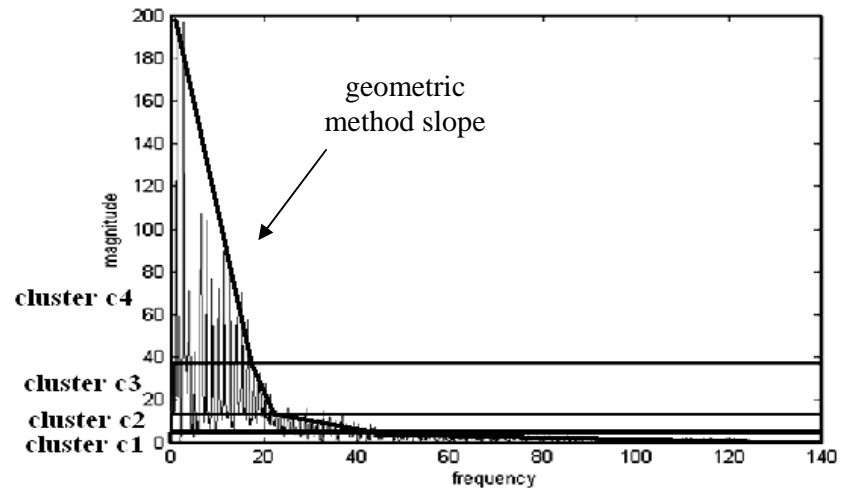
Fig. 3. ECG signal drift attenuation. (a) Original ECG signal; (b) ECG signal frequency spectrum; (c) Baseline drift extracted by moving median algorithm; (d) Conventional baseline drift attenuation with 1 Hz high-pass filter; (e) Baseline drift attenuation with moving median filter



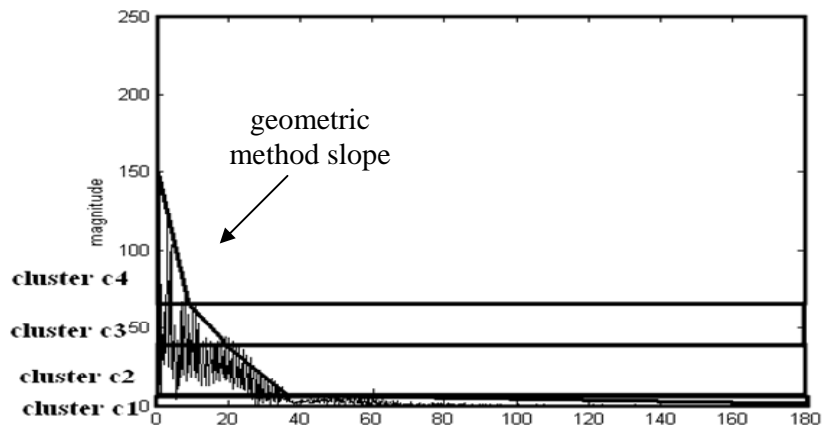
(a)



(b)

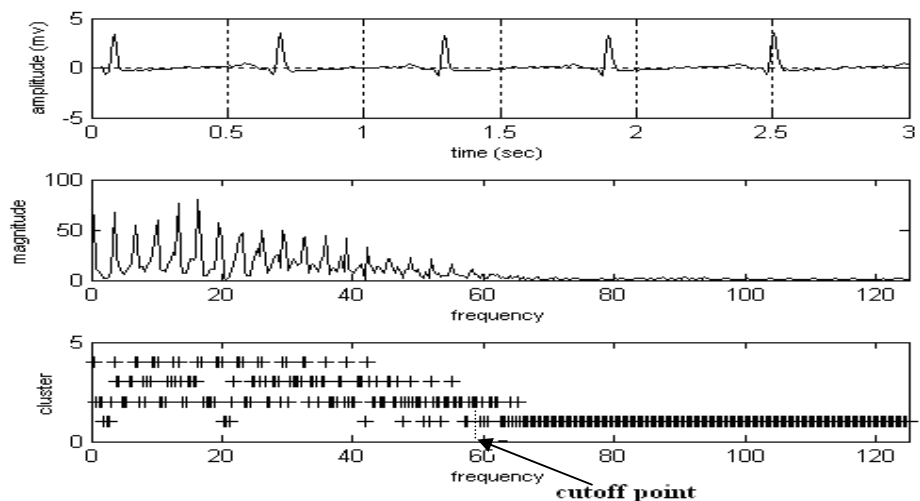


(c)

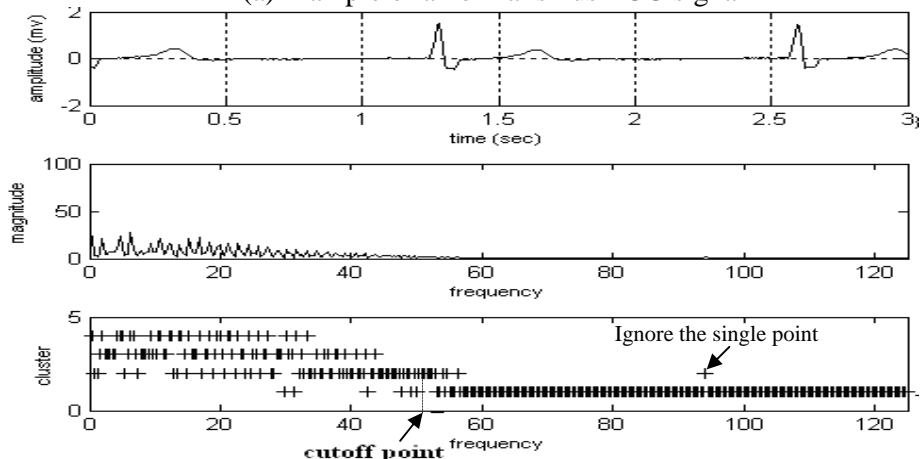


(d)

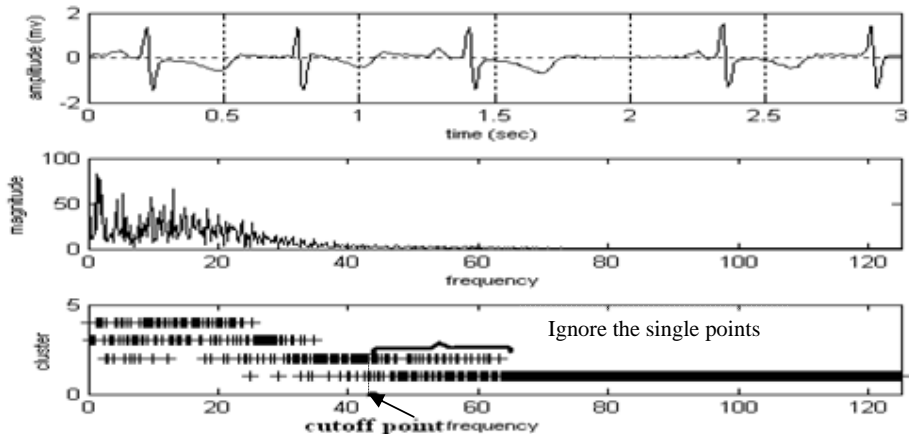
Fig. 4. Four typical ranges of amplitude for frequency spectrum in four classes of ECG (a) Normal sinus rhythm; (b) Supraventricular; (c) Atrial fibrillation; (d) Arrhythmia



(a) Example of a normal sinus ECG signal

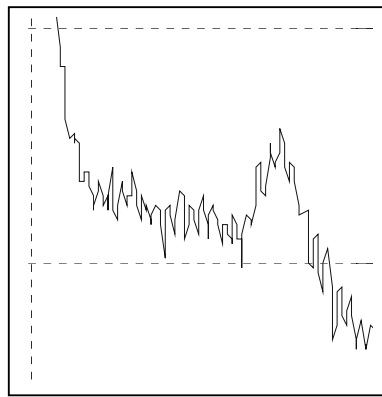


(b) Example of a supraventricular ECG signal

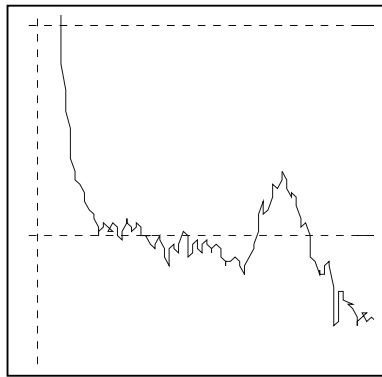


(c) Example of an atrial fibrillation ECG signal

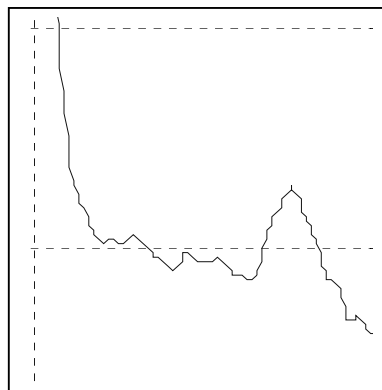
Fig. 5. Clustering the frequency spectrum. Top: ECG signal after baseline drift removal, Middle: Signal in frequency domain, Bottom: clustering of FFT



(a)



(b)



(c)

Fig. 6. Denoising by SOM based on the stable point (a) Original ECG signal; (b) Denoising by the first stable point; (c) Denoising by the second stable point

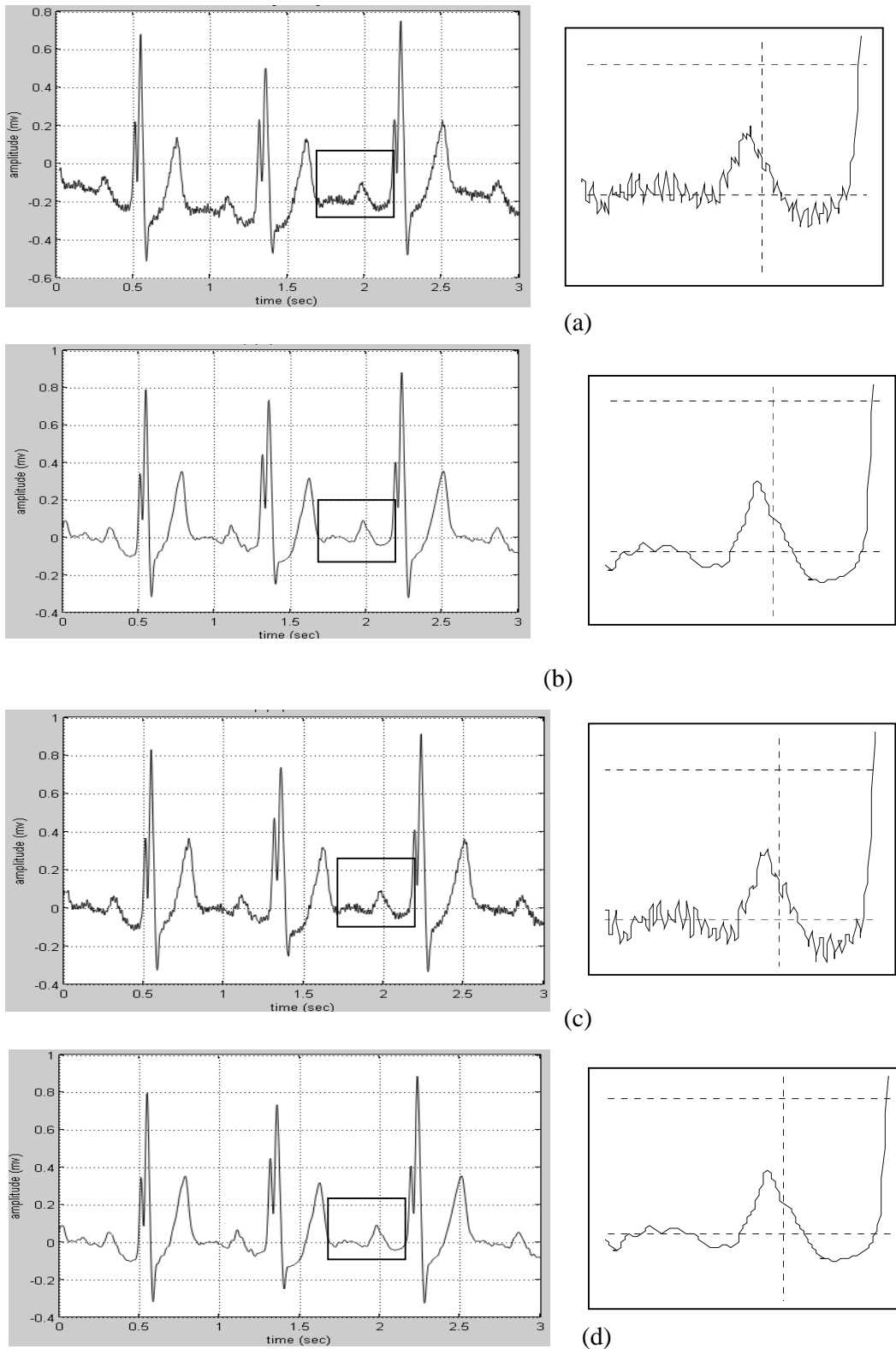


Fig. 7. Arrhythmia ECG signal. (a) Noisy ECG signal, (b) Denoised ECG signal by the automated calculated cutoff, (c) Denoised ECG signal by the classic cutoff (100 Hz), (d) Denoised ECG signal by the visually calculated cutoff. Enlarged portions of the signals are given on the right.

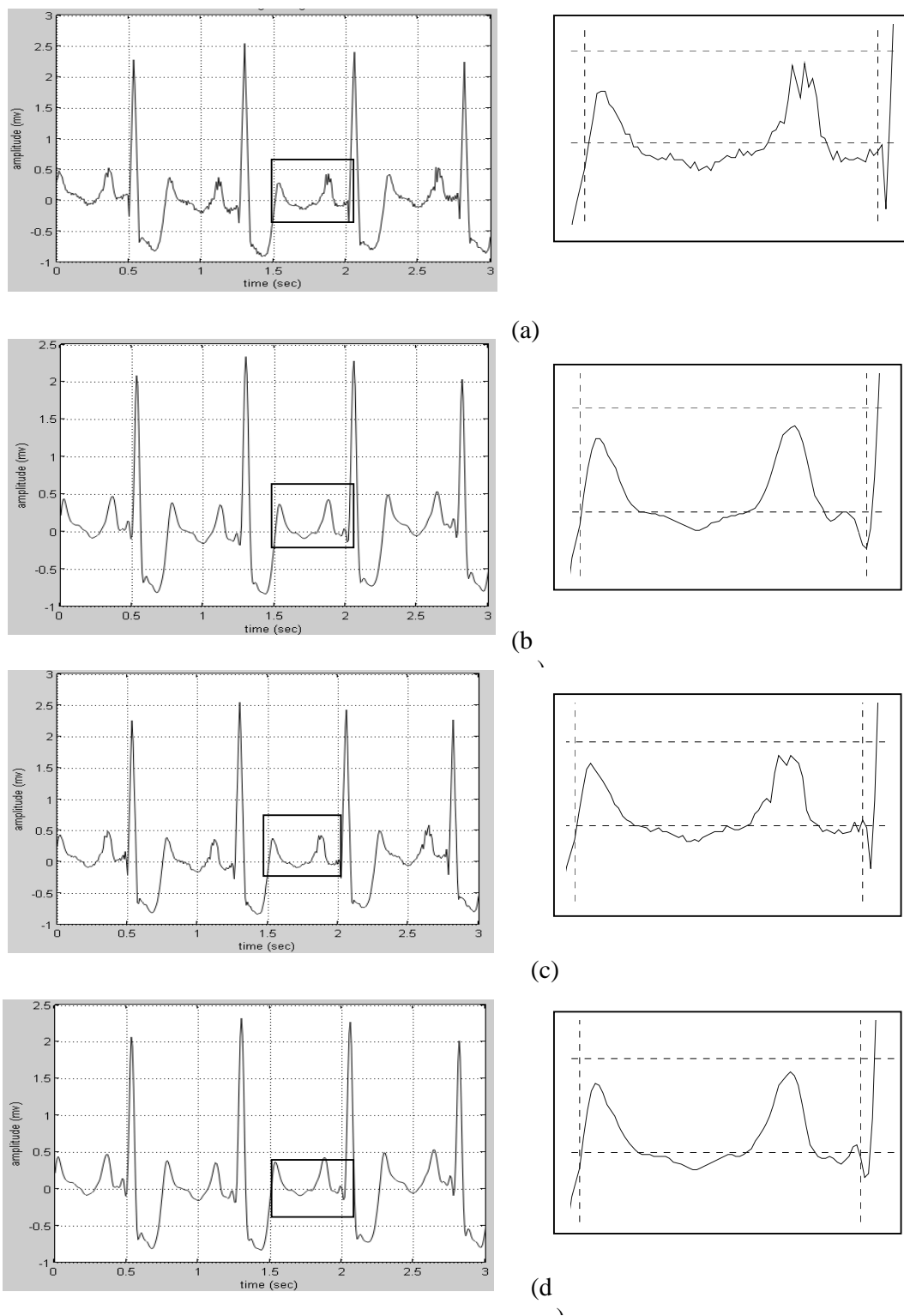


Fig. 8. Supraventricular ECG signal. (a) Noisy ECG signal, (b) Denoised ECG signal by the automated calculated cutoff, (c) Denoised ECG signal by the classic cutoff (100 Hz), (d) Denoised ECG signal by the visually calculated cutoff. Enlarged portions of the signals are given on the right.

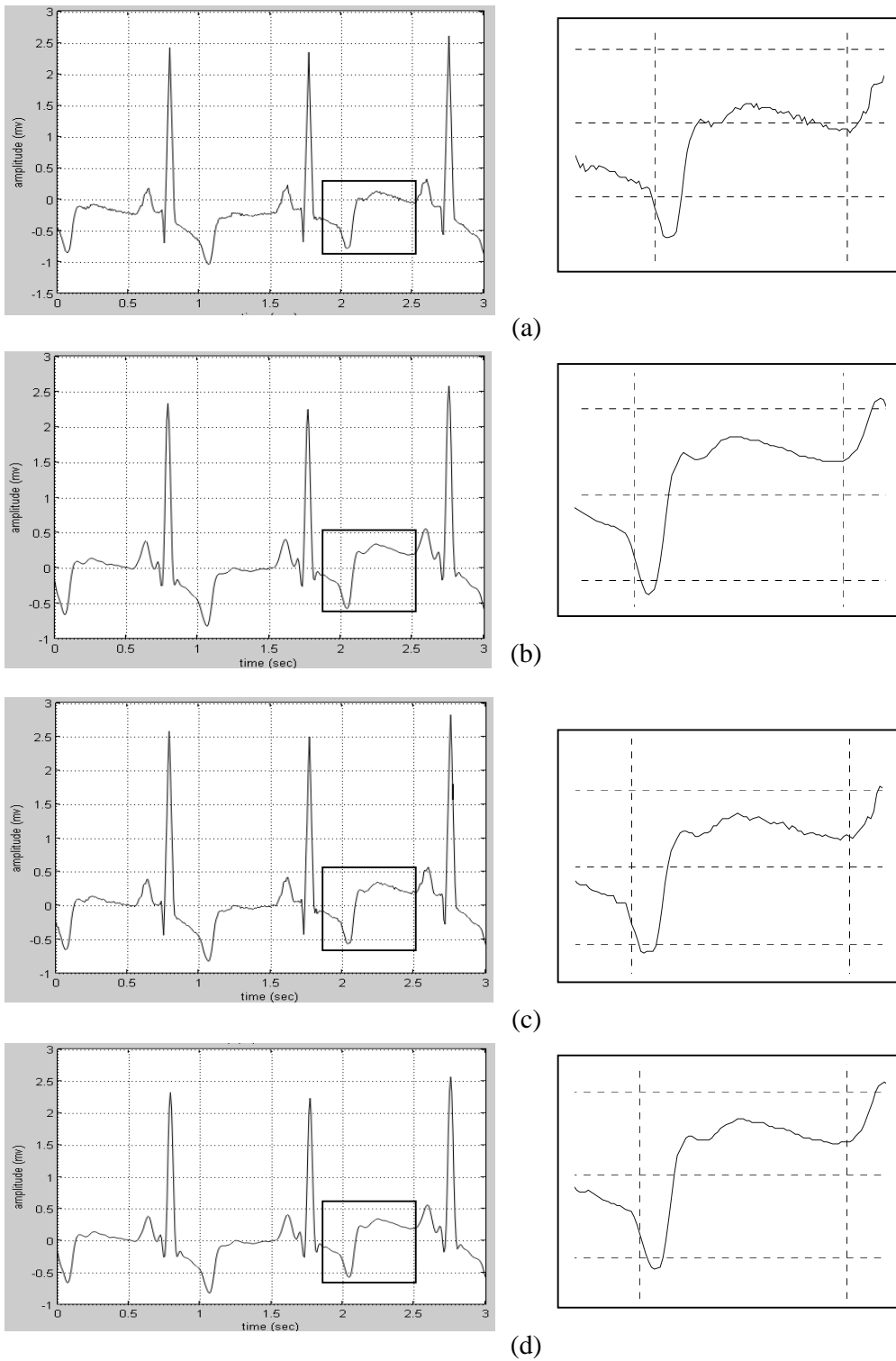


Fig. 9. Another supraventricular ECG signal. (a) Noisy ECG signal, (b) Denoised ECG signal by the automated calculated cutoff, (c) Denoised ECG signal by the classic cutoff (100 Hz), (d) Denoised ECG signal by the visually calculated cutoff. Enlarged portions of the signals are given on the right.

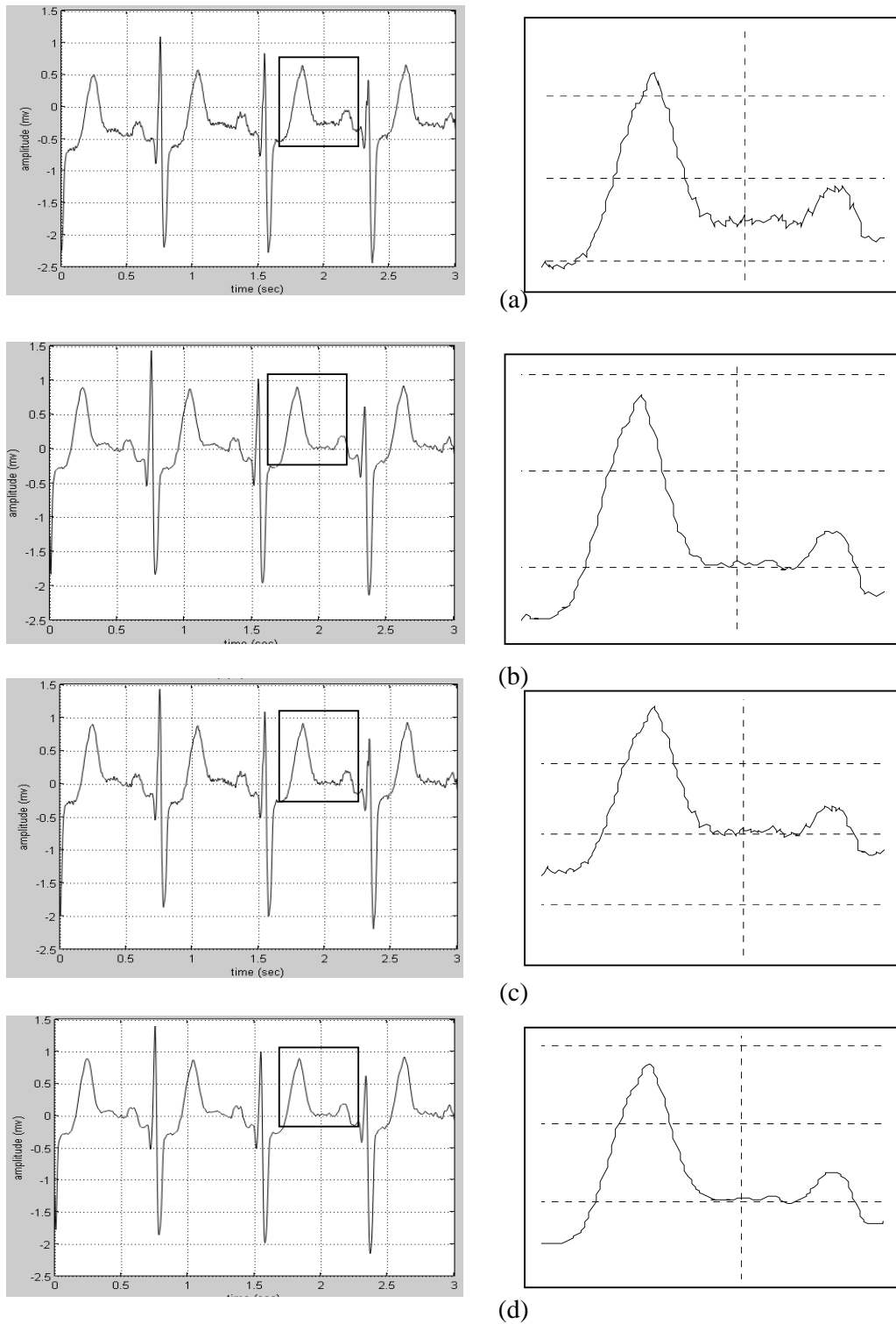


Fig. 10. Atrial fibrillation ECG signal. (a) Noisy ECG signal, (b) Denoised ECG signal by the automated calculated cutoff, (c) Denoised ECG signal by the classic cutoff (100 Hz) , (d) Denoised ECG signal by the visually calculated cutoff. Enlarged portions of the signals are given on the right.

Table 1. Typical ranges of amplitude (mv) for the four classes of ECG

	<b>C1</b>	<b>C2</b>	<b>C3</b>	<b>C4</b>	<b>Remark</b>
<b>normal sinus rhythm</b>	0-5	6-20	21-60	> 60	See Fig. 4(a)
<b>supraventricular</b>	0-1	2-4	5-10	> 10	See Fig. 4(b)
<b>atrial fibrillation</b>	0-5	6-15	16-40	> 40	See Fig. 4(c)
<b>arrhythmia</b>	0-5	6-40	41-70	> 70	See Fig. 4(d)

Table 2. Results of SOM for identifying the cutoff frequency (in Hz)

No.	Test signal	Automated $\omega_c$	Visual $\omega_c$	Squared error
1	supraventricular (rec-800)	54.68	54.1	0.34
2	supraventricular (rec-801)	53.63	53.2	0.18
3	supraventricular (rec-802)	64.84	64.2	0.41
4	supraventricular (rec-805)	44.14	43.6	0.29
5	supraventricular (rec-806)	80.46	80.1	0.13
6	supraventricular (rec-807)	38.67	38.3	0.22
7	supraventricular (rec-808)	41.05	40.1	0.90
8	arrhythmia (rec-101)	43.21	42.4	0.66
9	arrhythmia (rec-111)	27.35	26.4	0.90
10	arrhythmia (rec-113)	42.50	41.6	0.81
11	arrhythmia (rec-115)	32.51	31.9	0.37
12	arrhythmia (rec-116)	32.90	32.1	0.64
13	atrial fibrillation (rec-iaf1-ivc)	42.80	42.3	0.25
14	atrial fibrillation (rec-iaf2-ivc)	45.60	44.8	0.64
15	atrial fibrillation (rec-iaf6-ivc)	24.20	23.6	0.36
16	atrial fibrillation (rec-iaf13-ivc)	35.20	35.1	0.01
17	normal (rec-16483)	69.53	68.8	0.53
18	normal (rec-16420)	82.81	82.1	0.50
19	normal (rec-16773)	55.46	54.6	0.74
20	normal (rec-16273)	62.10	62.1	0.81
<b>MSE</b>				<b>0.48</b>